Crystal structure of engineered ACE2 complexed with SARS-CoV-2 Spike RBD

The coronavirus disease (COVID-19) caused by severe acute respiratory syndrome coronavirus 2 (SARS-CoV-2) has become a global pandemic and has tremendously affected on our lives. Infection by SARS-CoV-2 is initiated by its binding to angiotensin-converting enzyme II (ACE2) on the surface of human cells via the viral spike protein; therefore, inhibiting the binding of spikes to ACE2 is one of the most promising therapeutic strategies against COVID-19. A number of monoclonal antibodies that bind to spikes, especially the receptor binding domain (RBD), and block ACE2 engagement are currently in preclinical and clinical development. However, because of the high mutation rate of SARS-CoV-2, there is concern that the virus may acquire resistance to drugs and vaccines. An alternative molecule to antibodies in neutralizing SARS-CoV-2 is the extracellular region of ACE2, soluble ACE2 (sACE2) (Fig. 1) [1]. The main advantage of using the sACE2-based decoy receptor is its resistance to virus escape mutations. A virus mutant escaping from the sACE2 decoy should also have limited binding affinity to native ACE2 receptors on the cell surface, resulting in diminished or eliminated infectivity. In this study, we developed a SARS-CoV-2-neutralizing drug that overcomes viral mutations through protein engineering of ACE2 [2].

Since the affinity of wild-type (WT) sACE2 to RBD is not sufficiently high to be used for therapeutic purposes [3,4], we first attempted to modify ACE2 to increase its affinity (Fig. 1). We introduced mutations into ACE2 by a directed evolution method involving several rounds of random mutagenesis and cell sorting, and we obtained an ACE2 mutant, 3N39, which was judged to have an increased RBD binding activity on the basis of the cell-based binding assay results [2]. Sequence analysis revealed that seven mutations, A25V, K26E, K31N, E35K, N64I, L79F, and N90H, were introduced into ACE2(3N39). Quantitative measurements of binding affinity to RBD by surface plasmon resonance showed that the K_D value of WT sACE2 is 17.63 nM, whereas that of the 3N39 mutant is 0.29 nM, confirming that the RBD binding activity was, in fact, greatly enhanced by mutations. We further characterized each mutation and finally found that only four of the seven mutations (i.e., A25V, K31N, E35K, and L79F) were essential for affinity enhancement.

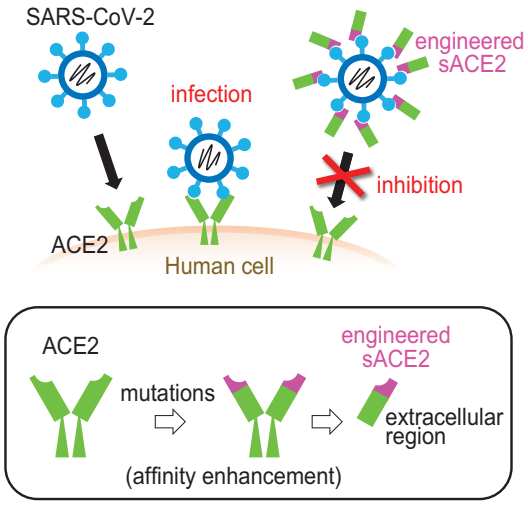

Fig. 1. Strategy for SARS-CoV-2 neutralization using engineered sACE2.

To understand the structural basis of the affinity enhancement, we next determined the crystal structure of the sACE2(3N39)-RBD complex. X-ray diffraction data were collected at SPring-8 **BL44XU**, and the structure was solved by molecular replacement at a final resolution of 3.2 Å. Structure refinement was promptly conducted, and the resulting model was deposited in PDB in December 2020 (PDB ID: 7dmu). This is the first SARS-CoV-2-related protein structure reported in Japan. From the crystal structure, it was confirmed that among the seven mutated residues in 3N39, the side chains of E26, I64, and H90, which were identified to have little or no contribution to the affinity enhancement, are exposed to solvent and not involved in either inter- or intra-molecular interactions (Fig. 2(a)). In contrast, four essential mutated residues were found to be involved in the formation of interaction sites for RBD in two regions. The first region consists of K31N and E35K mutation sites and is located at the center of the RBD binding interface. In the WT structure, E35 forms an intramolecular salt bridge with K31, making it unfavorable for direct intermolecular hydrogen bond formation with Q493 in RBD. In 3N39, simultaneous mutation of K31N and E35K resulted in the loss of this salt bridge, allowing K35 to exclusively form a direct intermolecular hydrogen bond with Q493 (Fig. 2(b)). The second region contains V25 and F79, both of which acquired larger hydrophobic side chains through mutations. These two residues, together with multiple hydrophobic residues, form a small hydrophobic pocket that accommodates F486 of RBD (Fig. 2(c)). WT ACE2 also has the corresponding pocket, but the L79F mutation in 3N39 makes the hydrophobic contacts more extensive. As for V25, it does not interact directly with F486 and may contribute to

improving the stability of the pocket by filling a space at the back of the pocket. Thus, the structure suggests that these four mutations collectively lead to the approximately 100-fold increase in the overall affinity.

Our crystal structure also provided a hint for designing an enzymatically inactive mutant of ACE2. Since the native ACE2 is an enzyme involved in blood pressure control, when sACE2 decoys are used as drugs, it may be better to eliminate their enzyme activity to prevent side effects. Interestingly, sACE2(3N39) in our crystal structure adopts a "closed" conformation where the enzymatic active site is completely inaccessible from the outside, which is quite different from the "open" conformation of the RBD-bound WT sACE2 structure reported so far (Fig. 3) [3,5]. As the residues mutated in 3N39 to improve affinity to RBD are far from the active site, we speculated that the closed conformation may be due to crystal packing. Then we introduced a double mutation, S128C/V343C, into ACE2(3N39) to fix this closed conformation with a disulfide bond.

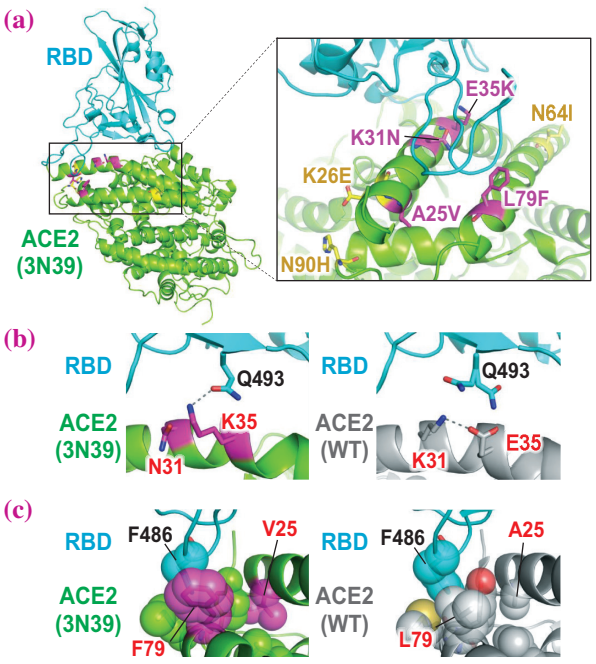

Fig. 2. Structural basis for the affinity enhancement of the ACE2(3N39) mutant. **(a)** Overall structure of the sACE2(3N39)-RBD complex. The essential and nonessential mutated residues for affinity enhancement are shown as magenta and yellow stick models, respectively. The expanded view of the RBD binding interface is provided in the inset. **(b)** Structures of the K31N/E35K mutation site in 3N39 (left panel) and its corresponding site in WT (right panel). Hydrogen-bonding interactions (within 3.0 Å) are indicated by dashed lines. **(c)** Structures of the A25V/L79F mutation site in 3N39 (left panel) and its corresponding site in WT (right panel). F486 residue of RBD and hydrophobic residues composing the F486-binding pocket of ACE2 are shown as stick models with transparent sphere models.

As expected, ACE2(3N39) with the S128C/V343C mutation completely lost its enzymatic activity without decreasing its affinity for RBD [2]. In addition, the introduction of this disulfide bond increased the T_m value of 3N39 by 7°C. The improvement in thermal stability should also be beneficial for pharmaceutical applications of the engineered ACE2.

The crystal structure confirmed that ACE2(3N39) binds to RBD through the same interface as WT ACE2, strongly suggesting a high resistance of our decoy drug to viral escape mutations. In fact, the SARS-CoV-2 escape mutation did not arise during culture in the presence of ACE2(3N39) [2]. Furthermore, we have already demonstrated the high therapeutic potency of ACE2(3N39) in a hamster model of COVID-19. These results indicate that ACE2(3N39)-based decoys can be effective therapeutic agents against various viral mutants. We are continuing our studies on engineered ACE2 with the aim of realizing its therapeutic application as soon as possible.

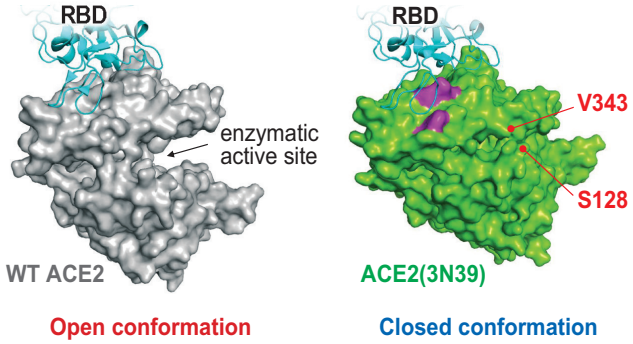

Fig. 3. Open and closed conformations of ACE2. The RBD-bound WT ACE2 (left, 6m0j) and the RBD-bound ACE2(3N39) (right) are shown as surface representations. The mutation sites in 3N39, which are essential for affinity enhancement, are shown in magenta.

Takao Arimori* and Junichi Takagi

Institute for Protein Research, Osaka University

*Email: arimori@protein.osaka-u.ac.jp

References

[1] W. Jing and E. Procko: Proteins **89** (2021) 1065.
[2] *Y. Higuchi, T. Suzuki, T. Arimori, N. Ikemura, E. Mihara, Y. Kirita, E. Ohgitani, O. Mazda, D. Motooka, S. Nakamura, Y. Sakai, Y. Itoh, F. Sugihara, Y. Matsuura, S. Matoba, T. Okamoto, J. Takagi, A. Hoshino: Nat. Commun.* ***12*** *(2021) 3802.*
[3] J. Shang *et al.*: Nature **581** (2020) 221.
[4] K.K. Chan *et al.*: Science **369** (2020) 1261.
[5] J. Lan *et al.*: Nature **581** (2020) 215.